Received: 3 March 2021 | Accepted: 10 March 2021

DOI: 10.1002/prp2.770

ORIGINAL ARTICLE

Repeated exposure of house dust mite induces progressive airway inflammation in mice: Differential roles of CCL17 and IL-13

Ravi Malaviya[1] | Zhao Zhou[1] | Holly Raymond[1] | Josh Wertheimer[1] | Brian Jones[1] | Rachel Bunting[1] | Patrick Wilkinson[1] | Lohith Madireddy[1] | LeRoy Hall[2] | Mary Ryan[1] | Tadimeti S. Rao[1]

[1]Discovery Immunology, Janssen Research & Development, LLC, Spring House, PA, USA

[2]Drug Safety Sciences (L.R.) Janssen Research & Development, LLC, Spring House, PA, USA

Correspondence
Ravi Malaviya, Discovery Immunology. Janssen Research & Development, LLC, 1400 McKean Road, Spring House, PA 19477, USA.
Email: rmalaviy@its.jnj.com

Abstract

We conducted a systematic evaluation of lung inflammation indued by repeated intranasal exposure (for 10 consecutive days) to a human aeroallergen, house dust mite (HDM) in BALB/c mice. Peak influx of neutrophils, monocytes/lymphocytes, and eosinophils was observed in bronchoalveolar lavage (BAL) on days 1, 7 and 11, respectively, and normalized to baseline by day 21. Peak elevations of Th2, myeloid-derived cytokines/chemokines and serum IgE were seen both in BAL and lung tissue homogenates between days 7 and 11, and declined thereafter; however, IL-33 levels remained elevated from day 7 to day 21. Airway hyperreactivity to inhaled methacholine was significantly increased by day 11 and decreased to baseline by day 21. The lung tissue showed perivascular and peribronchial cuffing, epithelial hypertrophy and hyperplasia and goblet cell formation in airways by day 11, and resolution by day 21. Levels of soluble collagen and tissue inhibitors of metalloproteinases (TIMP) also increased reflecting tissue remodeling in the lung. Microarray analysis demonstrated a significant time-dependent up-regulation of several genes including IL-33, CLCA3, CCL17, CD4, CD10, CD27, IL-13, Foxa3, IL-4, IL-10, and CD19, in BAL cells as well as the lung. Pretreatment of HDM challenged mice with CCL17 and IL-13 antibodies reduced BAL cellularity, airway hyper-responsiveness (AHR), and histopathological changes. Notably, anti-IL-13, but not anti-CCL17 monoclonal antibodies (mAbs) reduced BAL neutrophilia while both mAbs attenuated eosinophilia. These results suggest that CCL17 has an overlapping, yet distinct profile versus IL-13 in the HDM model of pulmonary inflammation and potential for CCL17-based therapeutics in treating Th2 inflammation.

KEYWORDS
airway inflammation, CCL17, house dust mite, IL-13

Abbreviations: AHR, airway hyper-responsiveness; BALF, bronchoalveolar lavage fluid; BSA, bovine serum albumin; CCL17, Chemokine (C-C motif) ligand 17; EPO, erythropoietin; G-CSF, granulocyte-colony stimulating factor; H&E, hematoxylin and eosin; HDM, house dust mite; IFN, interferon; IL, interleukin; mAb, monoclonal antibody; MCP-1, monocyte chemotactic protein-1; ME, mercaptoethanol; OVA, ovalbumin; PBS, phosphate-buffered saline; PHA, phytohemagglutinin; RANTES, regulated on activation, normal T cell expressed and secreted; TARC, thymus and activation regulated chemokine; TNF, tumor necrosis factor.

1 | INTRODUCTION

More than 300 million people worldwide suffer from allergic asthma characterized by variable and reversible airway obstruction, airway inflammation, remodeling, eosinophil recruitment, inflammation, mucus production, and AHR.[1] Among others, the $CD4^+$ T-helper cell type 2 (Th2) cell, activated in an antigen-specific manner, has emerged as an orchestrator of the inflammatory response to many allergens.[2–5]

House dust mites (HDM; *Dermatophagoides* sp.) are one of the most common sources of airborne allergens worldwide affecting more than 15%–20% of the population from industrialized countries.[6] Atopic patients exposed to HDM allergens develop Th2 inflammatory diseases such as allergic asthma, perennial rhinitis, and atopic dermatitis [(AD; 7].

CCL17 also known as TARC (thymus and activation regulated chemokine), is important for the development of airway inflammation in asthma through the recruitment of Th2 cells, Th17 cells, mast cells and iNKT, monocyte and dendritic cells.[8,9] In the lung, CCL17 is produced by both immune (e.g., monocytes, dendritic cells) and structural cells (e.g., epithelial cells and fibroblasts; 9). CCL17 is elevated in the airways of asthmatics and its receptor, CCR4, is expressed on numerous inflammatory cell types involved in the pathogenesis of allergic asthma, including Th2 cells, Th17 cells and iNKT cells. CCR4 is also present on structural cells in the lung, such as airway epithelial cells and smooth muscle cells, suggesting a pleiotropic role for CCL17 in airway biology. The precise role of CCL-17 pathway in HDM induced allergic inflammation is not well established.

Emerging evidence suggests that the nature of the cellular and molecular networks driving Th2 lung inflammatory response to HDM are complex and involve a multifaceted interplay between innate and adaptive immune mechanisms, and multiple cells in the lung. HDM activates the immune system through pattern recognition receptors[10] and via its proteolytic activity.[11] HDM induced lung inflammation in mice shares many pathological features with persistent human asthma, notably eosinophilic airway inflammation, mucus hypersecretion, fibrosis of the airway wall and AHR to inhaled methacholine.[12] Many HDM models published to date, have largely focused on mediators in the allergic response at the end of HDM exposure and provide only a snapshot of a complex and dynamic disease process. However, the relationship between critical inflammatory mediators, inflammatory and regulatory cells, AHR and inflammatory genes have not yet been carefully explored during the evolution. To the best of our knowledge, this is the only study in the literature exploring the development of HDM-induced acute inflammatory responses at various stages of the disease in mouse model of allergic asthma. The aims of the present study were to: (1) characterize the development and resolution of lung inflammation and AHR during repeated HDM exposure to further understand cellular and molecular pathways, and (2) explore impact of neutralization of CCL17 or IL-13 in this model.

2 | MATERIALS AND METHODS

2.1 | Mice

Female BALB/c mice (5- to 7-week old; Taconic farms) were housed in a controlled environment (12-h light/12-h dark photoperiod, 22°C ± 1°C, 60% ± 10% relative humidity). Mice were provided free access to autoclaved pellet food and tap water.

2.2 | Reagents

HDM was purchased from Greer Laboratories (Lenoir, NC, USA; batch number 129458). Methacholine, phosphate buffered saline (PBS), Eosin, Hematoxylin, Giemsa stain, formalin, ethanol, beta-mercaptoethanol (β-ME), and bovine serum albumin (BSA) were purchased from Sigma/Aldrich Chemical Co.

2.3 | HDM asthma model

Purified HDM extract (2 mg/ml in PBS; 25 µl/mouse/day) or PBS (25 µl/mouse/day) was administered intranasally to female BALB/c mice, once a day, for 10 consecutive days under isoflurane anesthesia (Figure 1) or animals were sacrificed before (day 1), during (day 2/7) and after the HDM (day 11/21) administration and their lungs were thoroughly lavaged with 3 volumes (0.75 ml each) of ice-cold PBS

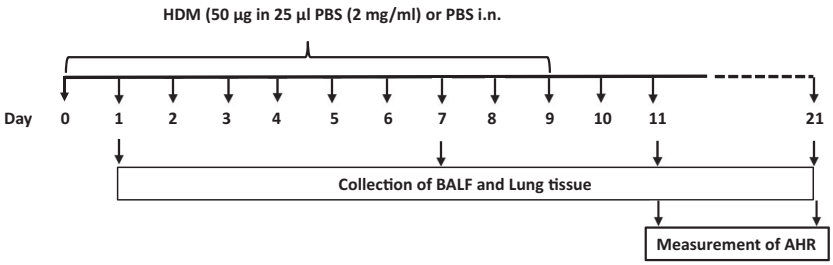

FIGURE 1 Mouse model of HDM challenge. Female BALB/c mice, 5–7 weeks old were exposed to HDM extract intranasally for 10 consecutive days under inhaled anesthesia. Control mice received PBS in the similar fashion. BALF and lungs were collected on days 1 (before HDM administration), 2, 7 (during HDM administration) and 11 and 21 (post HDM administration). AHR were measured on days 11 and 21

containing 0.1% bovine serum albumin (BSA). The pooled lavage was processed for leukocyte counts and cytokine analysis.[13] Lavage fluid was centrifuged (500*g*/5 min) supernatant saved at −80°C for analysis of inflammatory mediators, and the cell pellet was resuspended in saline containing 0.1% BSA to yield a final cell concentration of 0.1×10^6 cells/ml. Cytospin smears made from the cell suspension were stained with Giemsa for differential cell counts. Animals were perfused with saline and their lungs were collected for measurement of inflammatory mediators, soluble collagen levels, and RNA and histological analysis. Serum was collected for total IgE analysis.

2.4 | Treatment with anti-CCL17 and anti-IL-13 mAbs

Anti-CCL17, anti-IL-13 or isotype controls (Janssen R&D) (2 mg/kg each) were administered intraperitoneally on days 1, 5, and 9.

2.5 | Measurement of airway hyperresponsiveness

At the specific termination points after repeated HDM or saline administration, mice were anesthetized, tracheostomized, and connected to a Flexivent (Module 1, flexiVent, SCIREQ) instrument. Mechanical ventilation was set at 150 breaths/min with a tidal volume of 10 ml/kg and positive end expiratory pressure of 2–3 cm H_2O. Increasing concentrations of methacholine (10, 20 and 40 mg/ml) were delivered via an in-line nebulizer and the resulting, airway hyper-reactivity was measured approximately every 10 s for 2 min after each challenge. The dynamic lung resistance was calculated.

2.6 | Histological analysis of lungs

Lungs were inflated with 10% buffered formalin and then placed in 10% buffered formalin. After routine paraffin embedding, 5-µm sections were stained with H&E. To examine changes in mucus production and goblet cell hyperplasia, sections were stained Mason's trichrome and Periodic Acid Schiff (PAS). All histopathological analyses were conducted by an in-house veterinary pathologist, blinded to the treatments. Stained lung sections were graded on a semi-quantitative scale of 0–5, with 0 representing no relevant pathology finding and 5 representing the most severe grade changes relative to controls.

2.7 | Microarray analysis

For gene expression profiling, cell pellets from 0.5 ml of pooled lavage were suspended in 350 µl of RNA Later™ containing β-ME and frozen. Total mRNA extracted from the cell pellets with an RNeasy Mini kit (Qiagen), and reversed transcribed with a High Capacity cDNA Reverse Transcription Kit (Applied Biosystems) Standard curves were generated by serial dilutions from pooled cDNA samples. Real time PCR was performed with SYBR Green PCR Master Mix (Applied Biosystems) on an Applied Biosystems 7300HT real time PCR system. Glyceraldehyde 3-phosphate dehydrogenase (GAPDH) was used as a house keeping gene to normalize the data. Full-length coding sequences were obtained from the NCBI Gene Bank and primers were designed with Primer Express 3.0 software (Applied Biosystems).

Microarray procedure was performed according to the manufacturer's instructions. Hybridization to Affymetrix GeneChip HT MG430PM array plates and processed on a GeneTitan workstation following the manufacturer's protocol. The fold changes were calculated as the ratio of the expression level in each cell type versus the second highest expression level in all cell types. We focused on the genes that showed statistically significance of $p \leq .5$ with ≥1.5-fold up or down from controls.

2.8 | Quantitation of soluble collagen

Lung collagen content was assessed as per Biocolor assay (Biocolor). Briefly, lung tissue was homogenized in a 1 ml ice-cold lysis buffer and the homogenate was centrifuged at 13,000*g* for 30 min at 4°C. Next, 60 µl supernatant was mixed with 240 µl of 0.5 M acetic acid and 1 ml Sircol dye (Biocolor) for 30 min at room temperature on an orbital shaker. The resulting mixture was centrifuged at 13,000*g* for 10 min and the pellets were solubilized in 1 ml alkali reagent. Aliquots (200 µl) were transferred to a 96-well microtiter plate and the optical density (O.D.) was read at 540 nm. The collagen content was normalized to the weight of the lung.

2.9 | Analysis of inflammatory mediators

Lung tissues were homogenized in cold HBSS (pH 7.4 containing protease inhibitor cocktail, Roche Diagnostics), centrifuged (800*g* for 10 min) and the supernatants were collected. Cytokine concentrations were normalized to total protein assessed by BCA kit (Pierce). BALF and lung homogenate chemokine levels were measured using paired antibodies for murine TARC/CCL17, MDC/CCL22, eotaxin-1/CCL11, eotaxin-2/CCL24, MCP-1/CCL2 and RANTES/CCL5 (R&D Systems) in standardized sandwich ELISAs according to the manufacturer's protocol. Kits to measure IL-13 were purchased from R&D Systems. IL-4, IL-5, IFN-γ and KC/CXCL1 were measured in BAL and lung homogenate by MSD multiplex kit for mouse pro-inflammatory cytokines (Mesoscale Discovery), according to manufacturer's instruction.

2.10 | Data analysis

Data were analyzed using ANOVA followed by Mann–Whitney *U* Test. Data are presented as mean ± SEM. *p* values <.05 were taken as significant.

2.11 | Nomenclature of targets and ligands

Key protein targets and ligands in this article are hyperlinked to corresponding entries in http://www.guidetopharmacology.org, the common portal for the data from the IUPHAR/BPS Guide to PHARMACOLOGY[14] and are permanently achieved in the Concise Guide to PHARMACOLOGY 2019/20.[15]

3 | RESULTS

3.1 | Kinetics of cellular influx in the lungs of HDM treated mice

The time course of HDM model is depicted in Figure 1. Repeated exposure of HDM induced robust influx of inflammatory cells into

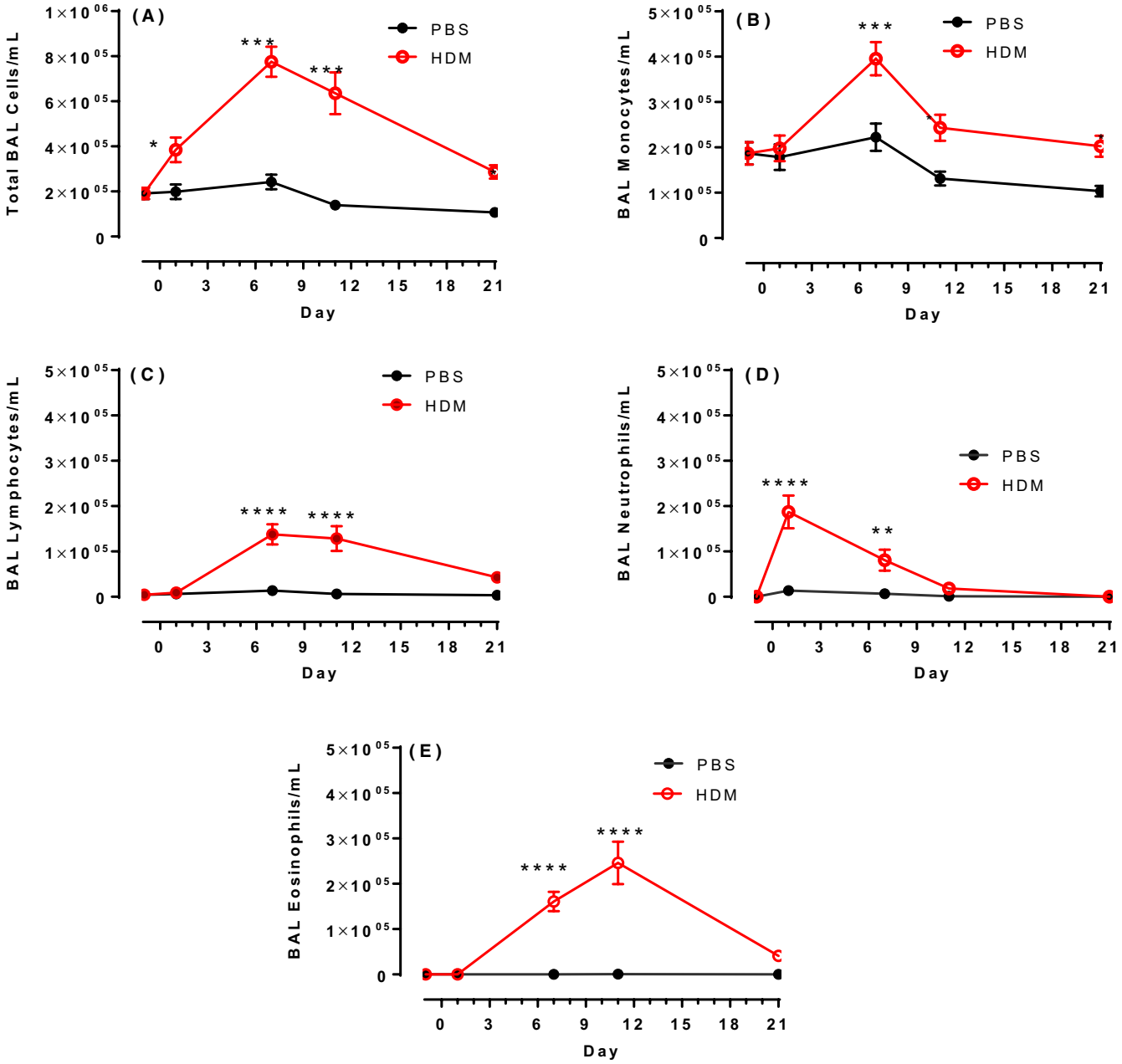

FIGURE 2 Kinetics of Leukocyte profile in bronchoalveolar lavage after HDM challenged mice. Mice were intranasally administered with PBS or HDM once daily for 10 consecutive days (day 0–day 9). At times indicated lungs of the mice were lavaged and total leukocytes (A), monocytes (B), lymphocytes (C), neutrophils (D), and eosinophils (E) were counted. The results are expressed as cells/ml. The data points are represented as mean ± SEM. $N = 6$ mice/group. $^{*}p < 0.05$; $^{**}p < 0.01$; $^{***}p < 0.001$ and $^{****}p < 0.0001$ compared with PBS challenged group as determined by the two-way ANOVA-Bonferroni test

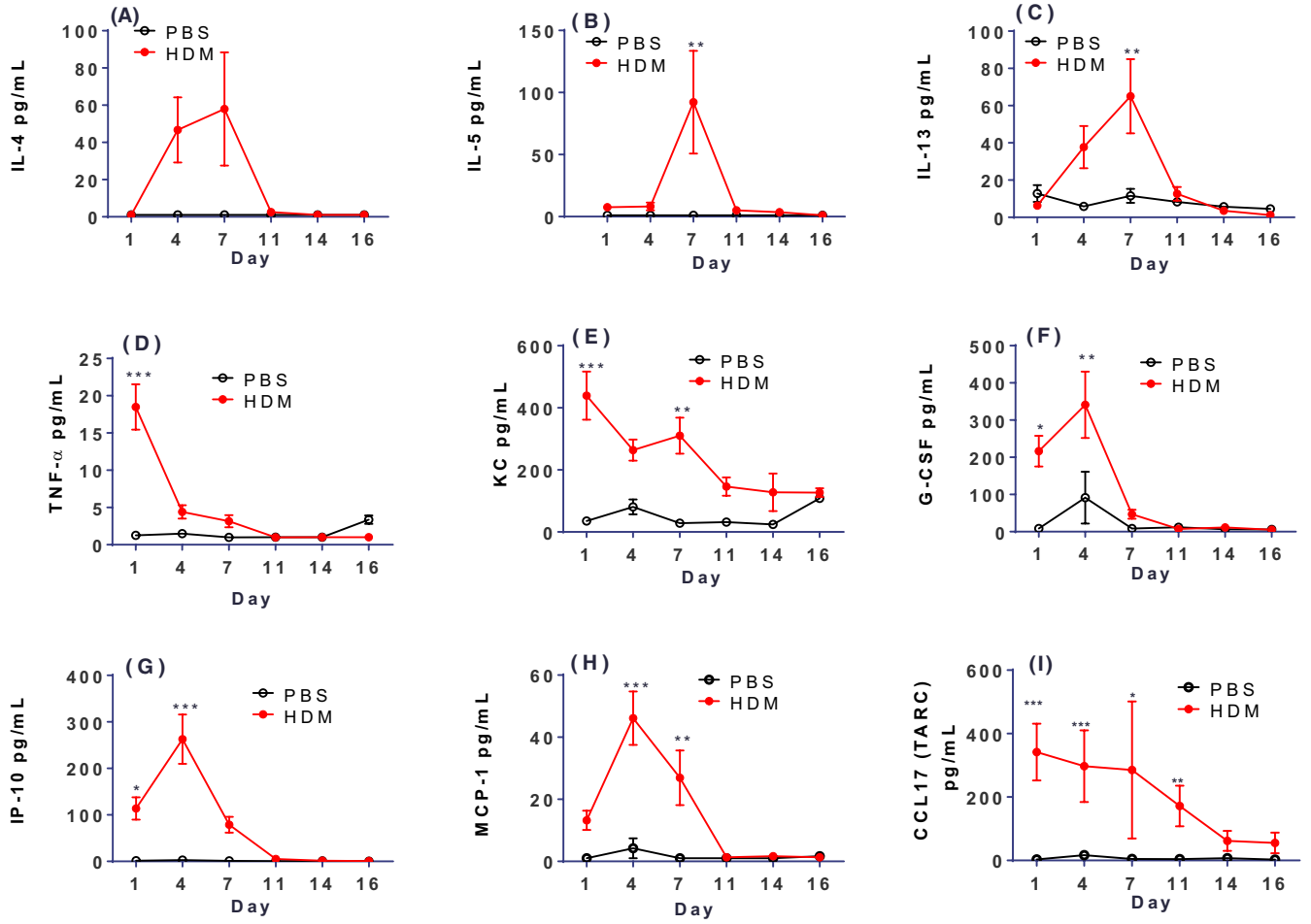

FIGURE 3 Kinetics of profile of inflammatory mediators in bronchoalveolar lavage after HDM challenge. Mice were intranasally administered with PBS or HDM once daily for 10 consecutive days (day 0 to day 9). At times indicated lungs of the mice were lavaged and IL-4 (A), IL-5 (B), IL-13 (C) TNFα (D) KC (E) G-CSF (F) IP-10 (G) MCP-1 (H) and CCL17 (I) were measured in the bronchoalveolar lavage fluids of PBS and HDM challenged mice. The results are expressed as pg/ml. The data points are represented as mean ± SEM. $N = 6$ mice/group. $^{*}p < 0.05$; $^{**}p < 0.01$ and $^{***}p < 0.001$ compared with PBS challenged group as determined by the two-way ANOVA-Bonferroni test

the airway lumen (Figure 2). The total BAL cellularity and number of lymphocytes increased as early as 24 h, with a peak response by day 7 followed by gradual decline by day 21 (Figure 2A and C). Monocyte levels increased slowly; peak increases in monocytes were seen by day 7 and decreased to near baseline levels by day 21 (Figure 2B). In contrast, peak neutrophilia observed as early as 24 h was normalized by day 21 (Figure 2D). BALF eosinophils, however showed a delayed increase with a peak on day 11 and were back to baseline by day 21. (Figure 2E). Thus, HDM challenge trigged influx of myeloid and lymphoid cells in the airway lumen of mice with distinct kinetics.

3.2 | Kinetics of BAL fluid cytokines in the lungs of HDM treated mice

Th2 cytokines, IL-4, IL-5, and IL-13 were significantly elevated in the BAL fluids (BALF) of HDM challenged mice (Figure 3A–C). Levels of IL-4 and IL-13 were significantly elevated over baseline by day 4, peaked at day 7 and subsided by day 11–14. IL-5, on the other hand, showed delayed increases (Figure 3B), with a peak at day 7 and reached nadir by day 11. Thus, changes in IL-5 preceded eosinophilic influx. BALF levels of TNFα, KC, G-CSF, IP-10, and MCP-1 were significantly elevated as early as day 1, showed a peak response by day 4 (Figure 3D–H) and declined thereafter. Interestingly, BALF CCL17 levels were significantly increased as early as day 1 and remained high until day 11, before declining to near baseline by day 14 (Figure 3I).

Because of the potential dilution of secreted mediators in BALF from the lavage process, many inflammatory mediators were either not detected or detected at low levels. We therefore evaluated cytokine levels in the lung homogenates of treated mice. Lung tissue levels of IL-4, IL-5, IL-13, and TARC (CCL17) increased by day 7 and decreased thereafter. In contrast, lung levels of IL-33 remained elevated from day 7 to day 21 (Figure 4A). Levels of IL-1α, IL-1β, IFN-γ, IL-17A, and TNFα were elevated by day 7 and normalized by day 21 (Figure 4B). Levels of interferon gamma-induced protein 10 (IP-10), KC, MCP-1, RANTES, and EPO increased by day 7 and generally normalized by day 21 (Figure 4C).

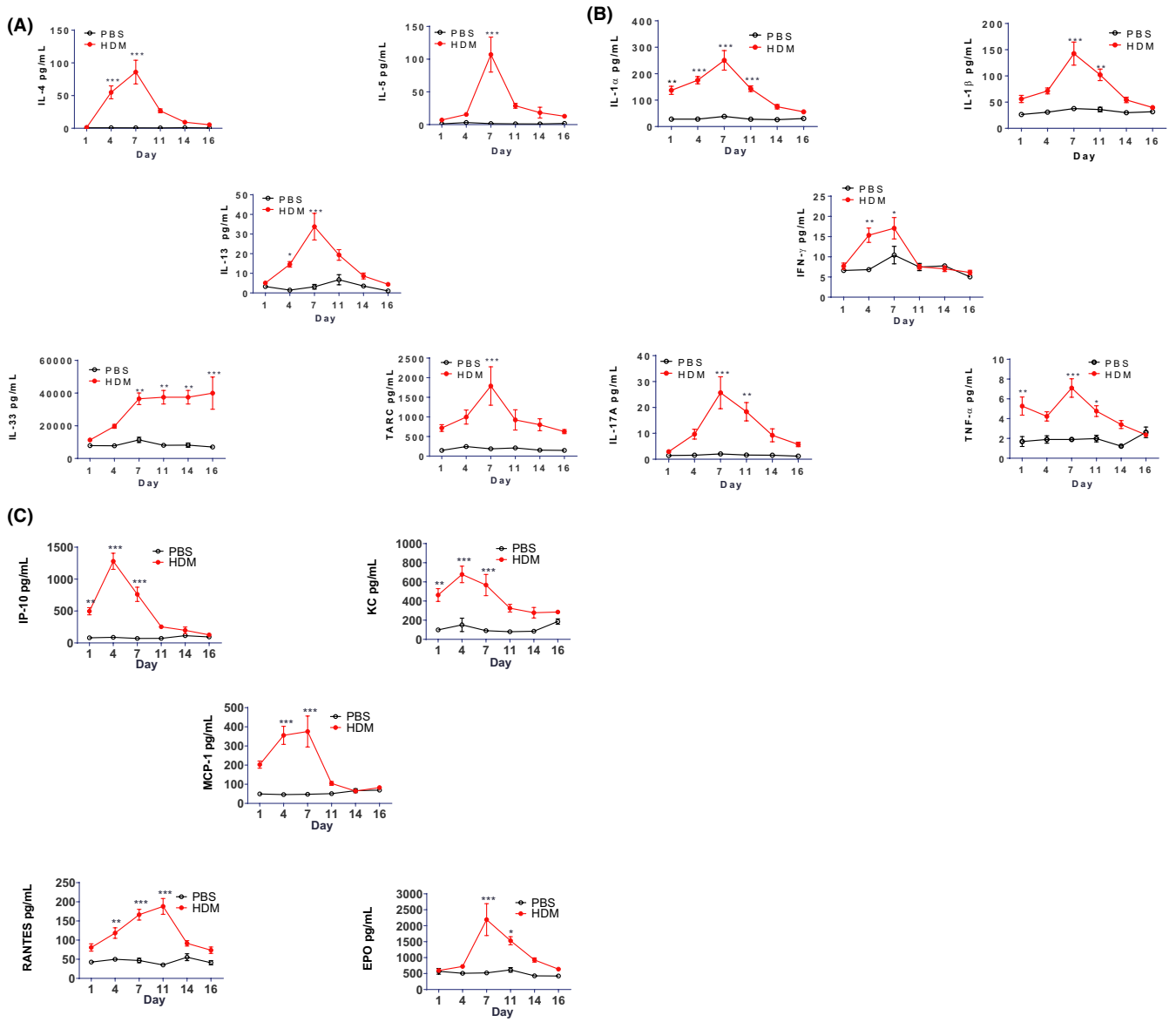

FIGURE 4 Kinetics of profile of inflammatory mediators in lung homogenate after HDM challenge. Mice were intranasally administered with PBS or HDM once daily for 10 consecutive days (day 0–day 9). At times indicated lungs of the mice were harvested, homogenized and various cytokine (A and B) and chemokine (C) levels were measured in the supernatants of lung homogenates of PBS and HDM challenged mice. The results are expressed as pg/ml. The data points are represented as mean ± SEM. $N = 6$ mice/group. $^{*}p < 0.05$; $^{**}p < 0.01$ and $^{***}p < 0.001$ compared with PBS challenged group as determined by the 2-way ANOVA-Bonferroni test

3.3 | Kinetics of plasma IgE levels in HDM treated mice

Serum IgE levels significantly increased by day 7, peak increases were seen by day 11 and declined to baseline levels by day 16 (Figure 5).

3.4 | Kinetics of airway hyper-responsiveness to methacholine in HDM challenged mice

Mice challenged with HDM for 10 days and challenged 24 h later with methacholine showed an exaggerated AHR response (Figure 6). The AHR response to methacholine was largely resolved by day 21 (Figure 6).

3.5 | Gene expression profile in the BAL cells and lung tissue of HDM challenged mice

A DNA microarray analysis was conducted to measure the expression levels of genes in the BAL cells and the lung tissue at various time points during (day 1 and 7) and after (day 11 and 21) HDM challenge and the results are summarized in Table 1. Differential gene expression between HDM and saline treated groups was seen both in the lung tissue and in BAL cells over the time course of the study. By day 11, 1433 and 1675 genes were differentially expressed in lung tissue and BAL cells, respectively. Interestingly, the BAL cells showed a more sustained differential gene expression even at day 21 of the study (10 days

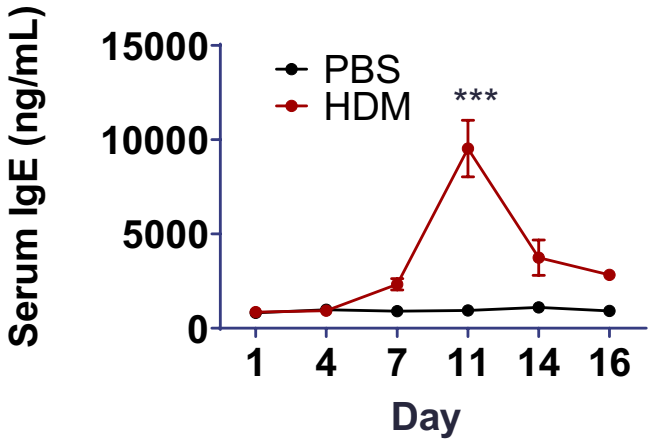

FIGURE 5 Kinetics of IgE profile in the serum of HDM challenged mice. Mice were intranasally administered with PBS or HDM once daily for 10 consecutive days (day 0–day 9). At times blood was collected from anesthetized mice and serum IgE levels were measured by ELISA. The results are expressed as ng/ml. The data points are represented as mean ± SEM. N=6 mice/group. ***$p < 0.001$ compared with PBS challenged group as determined by the two-way ANOVA-Bonferroni test

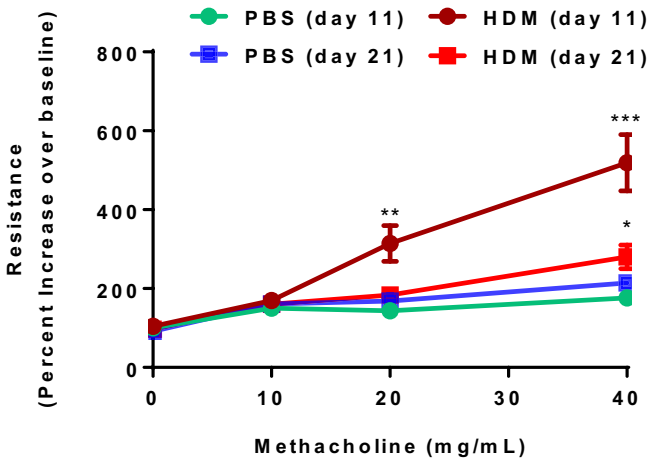

FIGURE 6 Airway hyper-responsiveness in HDM challenged mice. Mice were intranasally administered with PBS or HDM once daily for 10 consecutive days (day 0–day 9). At day 11 and 21 airway hyper-reactivity of mice to increasing doses of methacholine was measured by Flexivent. The results are expressed as percent increase in airway hyperreactivity over baseline. The data points are represented as mean ± SEM. $N = 6$ mice/group. *$p < 0.05$; **$p < 0.01$ and ***$p < 0.001$ compared with PBS challenged group as determined by the two-way ANOVA-Bonferroni test

post last HDM) whereas in the lung tissue, there was a precipitous drop between day 11 and day 21. In both compartments, proportionally more upregulated genes were seen relative to down regulated genes. We then focused on select group of most differentially expressed genes in BAL cells and lung tissue. At each time point, we explored gene expression changes in a comprehensive manner and a summary of DEG is presented in Tables S1–S8.

The genes with highest differentially expression in BAL cells were *IL-33*, *CLCA3*, *CCL17*, *CD4*, *IL-4*, *CD19*, and *CD27* (Figure 7). The corresponding genes in the lung tissue were *IL-13*, *CLCA3*, *IL-4*, *Foxa3*, *CD4*, *CD19*, and *IL-10* (Figure 8). It should be noted that expression of *CCL17* and *CD4* was induced as early as day 1 in the BAL unlike all other markers which were increased at day 7. The increased *IL-4* expression was validated by IL-4 protein levels in the BAL. Both in the lung tissue and BAL, *CLCA3* was the highest expressed gene, a gene involved in goblet cell function.

3.6 | Lung histopathology

HDM induced robust airway inflammation characterized by peribronchial and perivascular infiltrates mixed with eosinophils, neutrophils, and lymphocytes (Figure 9A–D). Examination of the time course of HDM exposure revealed a mild and acute perivascular inflammation on Day 1. By day 7, thick perivascular cuffs, bronchial epithelial hypertrophy and hyperplasia were observed (Figure 9G–H). Acute inflammatory cells were observed marginating underneath the endothelium in the perivascular space and there was subpleural thickening (Figure 9C). By day 11, the lungs developed perivascular edema and were full of multinucleated giant cells and eosinophils (Figure 9C). Goblet cell hypertrophy and hyperplasia were observed in the bronchioles (Figure 9E–F and I). The lung contained areas of multinucleated giant cell formation, alveolar emphysema, and acute bronchiolitis. By day 21, the bronchiolar epithelium in HDM group was similar to controls.

Overexpression of collagen is a hallmark of tissue remodeling and fibrosis. We thus examined the expression of collagen (Figure 10A), TIMP (Figure 10B) and pentraxin3 (PTX3) (Figure 10C) in the lung tissue at various time points during the HDM exposure. The total lung collagen content and TIMP were increased significantly after 7 days, then declined to near baseline by day 14. Lung PTX3 increased modestly and later during the HDM challenge (day 11).

TABLE 1 Lung and BAL cell gene analysis of HDM-challenged mice

Comparison PBS versus HDM challenge	Lung genes			BAL cell genes		
	Total	Up	Down	Total	Up	Down
Day 1	509	427	82	819	628	191
Day 7	1093	673	220	1023	824	199
Day 11	1433	1194	239	1675	994	681
Day 21	167	120	47	1142	803	339

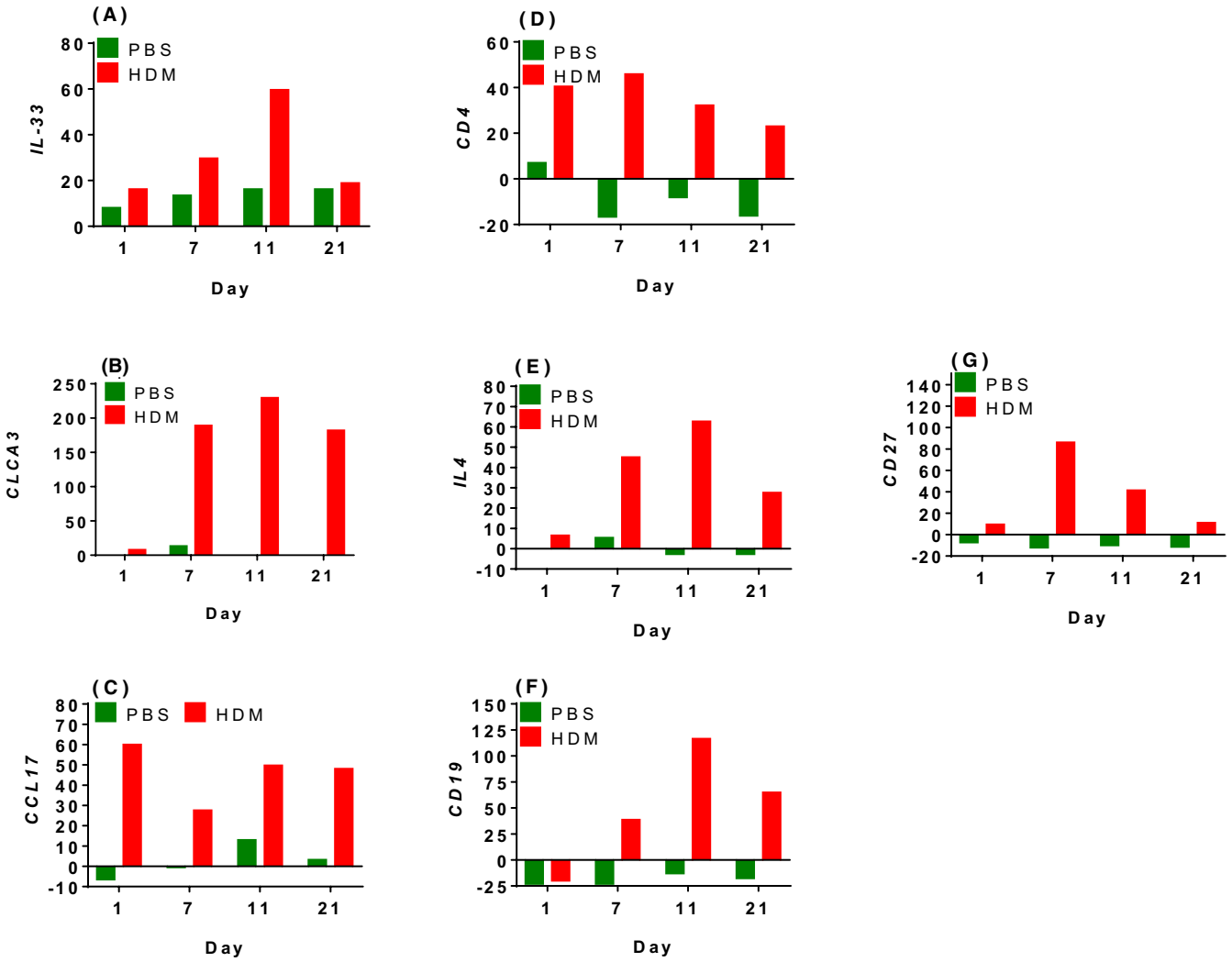

FIGURE 7 Expression of inflammatory genes in BAL cells after HDM challenge. Mice were intranasally administered with PBS or HDM once daily for 10 consecutive days (day 0 to day 9). At times BALF were harvested, and RNA was extracted for gene profiling. Expression of *IL-33* (A), *CLCA3* (B), *CCL17* (C), *CD4* (D), *IL-4* (E), *CD19* (F) and *CD27* (G) genes was quantified

3.7 | Effect of anti-CCL17 and anti-IL-13 on HDM-induced airway inflammation

As CCL17 and IL-13 levels are increased upon HDM challenge (Figures 3 and 4), we sought to explore the effects of neutralization of CCL17 or IL-13 on HDM-induced lung inflammation. To this end, mice were treated with anti-CCL17, IL-13, or isotype mAbs (days -1, 5, and 9; Figure 11A) and AHR and BAL cell influx were measured on day 11. A robust AHR response to methacholine was observed in isotype control treated mice. Both anti-CCL17 and anti-IL-13 treatments blunted the AHR response (Figure 11B). This reduction in AHR response was accompanied by attenuated cellular influx in the airway lumen of HDM challenged mice by both CCL17 and IL-13 mAbs (Figure 11C–E). Interestingly, while anti-IL-13 inhibited the influx of both eosinophils and neutrophils, anti-CCL17 only prevented influx of eosinophils (Figure 11D–E). At the histology level, IL-13 or CCL17 neutralization prevented hypertrophy and hyperplasia of bronchiolar epithelial cells and the formation of goblet cells (Figure 12). Qualitatively, a more significant attenuation of inflammation was seen with IL-13 neutralization versus CCl-17 neutralization.

4 | DISCUSSION

The HDM is a common household allergen, causally linked to the development of asthma in children and adults.[16,17] HDM exerts its inflammatory response via *Der p* 1, 3, 5, and 9 antigens by stimulating airway epithelium to produce Th1/Th2 inflammatory response through protease-activated receptor-2 mediated mechanism.[18–21] While there are several commercial HDM allergens, we utilized Greer extract in our studies as it is one of the most characterized[12,18,22] and induces pronounced increases in CCL20, CCL17 and interleukin 5 accompanied by HDM-specific IgE, goblet cell hyperplasia, eosinophilic inflammation and airway hyper-reactivity.[23] In the present study, we attempted to systematically characterize HDM-induced

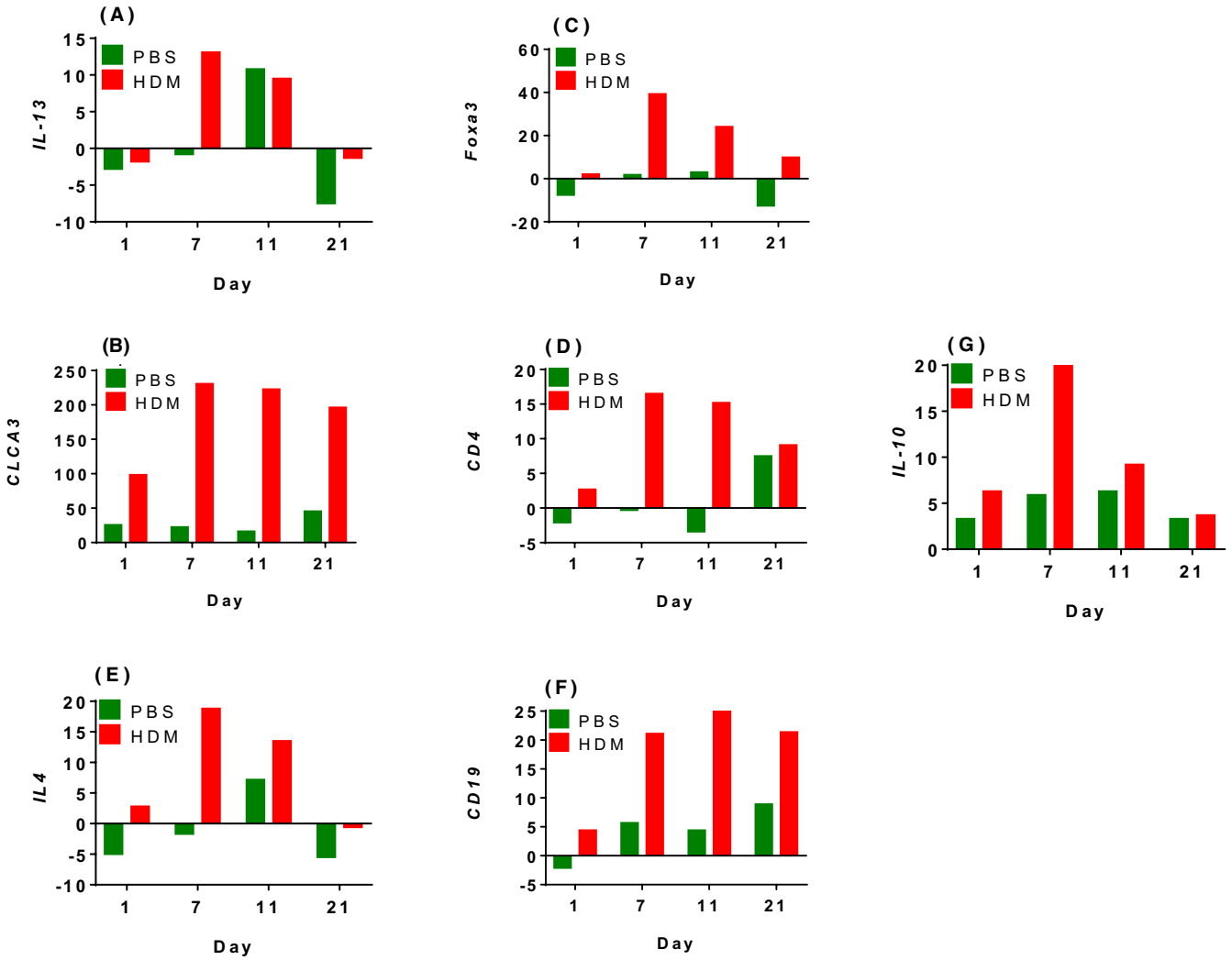

FIGURE 8 Expression of inflammatory genes in Lung tissue after HDM challenge. Mice were intranasally administered with PBS or HDM once daily for 10 consecutive days (day 0 to day 9). At times lung tissue were harvested, and RNA was extracted for gene profiling. Expression of *IL-13* (A), *CLCA3* (B), *Foxa3* (C), *CD4* (D), *IL-4* (E), *CD19* (F) and *IL-10* (G) genes was quantified

allergic airway inflammation at various stages following repeated exposure in BALB/c mice.

HDM exposure resulted in progressive airway inflammation characterized by recruitment of both myeloid and lymphoid cells into the airway lumen, elaboration of multiple cytokines (Th1, Th2, and Th17), differential gene expression with evidence of both histopathological and structural changes of the lungs. This inflammatory response is highly dynamic in nature with a progressive increase and resolves when HDM challenge is discontinued.

At the cellular infiltrate level, the airway inflammation was predominantly neutrophilic at the early stages and transitioned into an eosinophilic inflammation during the later days of HDM exposure, with the lymphoid cellular infiltration as the continuum in between. Both rodent and human studies have revealed that neutrophils are important in the pathobiology of asthma. These results are generally consistent with those seen under differing experimental conditions such as different strains of mice and HDM dose and/or duration of exposure.[12,18,24] Similar to murine studies, in human, randomized, double blind placebo control studies demonstrated that instillation of HDM with LPS results in significant neutrophil increase in the blood of asthmatics compared with placebo controls.[25,26]

The airway epithelial cells, the first cell type to be exposed to inhaled airborne allergens serve both as a passive barrier and a site for induction of the allergic response by microbial pathogen-associated molecular patterns (PAMPs) or to damage-associated molecular patterns (DAMPs) released upon tissue damage, cell death, or cellular stress. Multiple cytokines and chemokines induce the recruitment and the activation of DCs to promote Th2-biased airway inflammation through the inhibition of IL-12, the induction of chemokines as MDC/TARC which attract Th2 cells, or the overexpression of OX40L at the DC surface that can induce Th2 cell development. Epithelial-derived chemokines/cytokines also activate innate immune cells such as basophils, mast cells, and eosinophils to sustain the Th2 priming.[27–30]

The Th2- cytokines (IL-4, IL-13, IL-5) hallmarks of Th2 inflammation peaked around day 7, progressively declined during the course

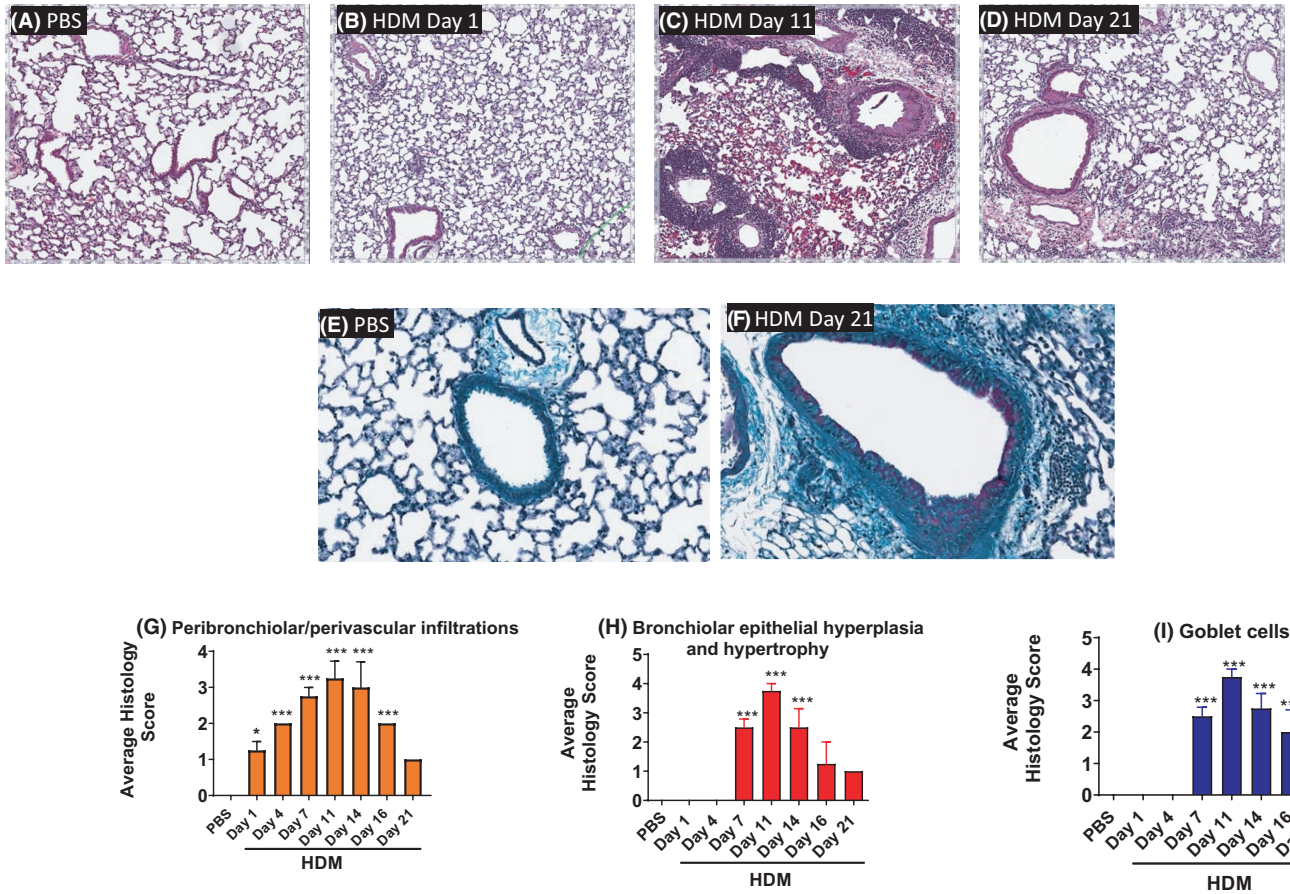

FIGURE 9 Kinetics of histopathological changed in HDM challenged mice. Mice were intranasally administered PBS or HDM once daily for 10 consecutive days (day 0–day 9). Lung tissues were obtained on times indicated and stained with hematoxylin and eosin (A–D) or PAS (E–F). Representative photomicrographs of airway sections are shown. (A–D) 10× magnification. (E–F) 40× magnification. Lung sections were scored for histopathologic changes. Peribronchial/perivascular infiltration of inflammatory cells (G), bronchiolar epithelial cell hyperplasia and hypertrophy (H) and increased goblet cell formation (I) were evaluated. The results are expressed on a scale of 0–5. The data points are represented as mean ± SEM. $N = 6$ mice/group. $^{*}p < 0.05$ and $^{***}p < 0.001$ compared with PBS challenged group as determined by the two-way ANOVA-Bonferroni test

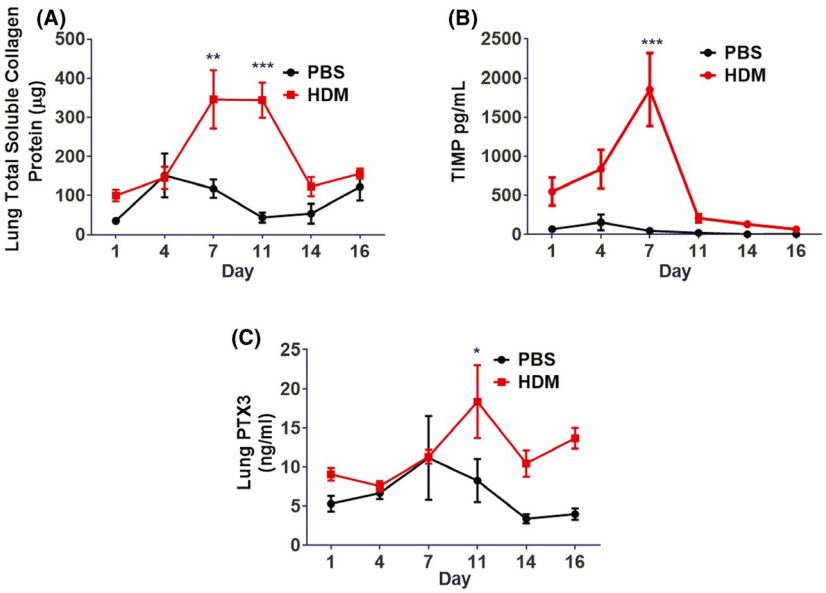

FIGURE 10 Increase in markers of airway remodeling after HDM challenge. Mice were intranasally administered with PBS or HDM once daily for 10 consecutive days (day 0–day 9). At times BALF and lung tissue were collected and lung tissue collagen (A). BALF TIMP (B) and lung tissue PTX3 (C) levels were measured. The results of lung collagen are expressed as µg/ml; PTX3 are expressed as ng/ml and TIMP are expressed as pg/ml. The data points are represented as mean ± SEM. $N = 6$ mice/group. $^{*}p < 0.05$; $^{**}p < 0.01$ and $^{***}p < 0.001$ compared with PBS challenged group as determined by the two-way ANOVA-Bonferroni test

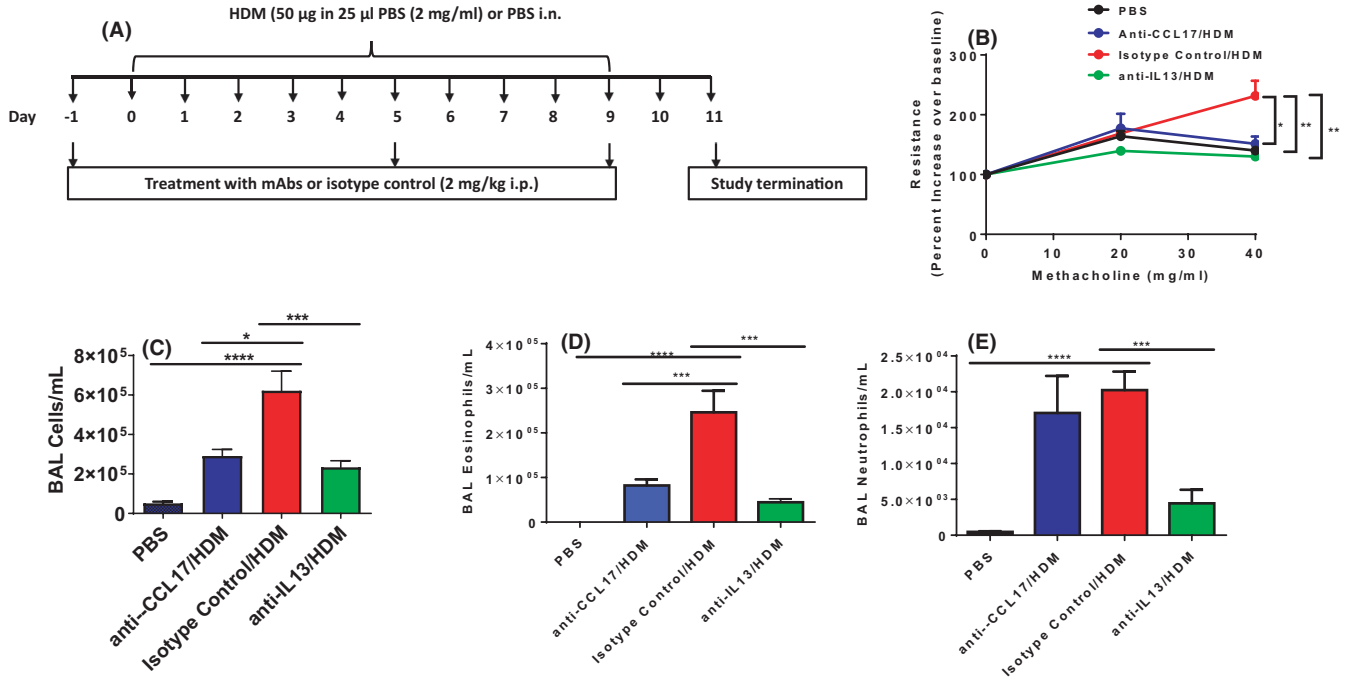

FIGURE 11 Effect of anti-CCL17 mAb on airway inflammation in HDM challenged mice. Mice were sensitized to PBS or HDM for 10 consecutive days (day 0–day 9). Mice were treated with 2 mg/kg of neutralizing anti mouse CCL17 or anti mouse IL-13 on days 1, 5, and 9 (A). At day 11 airway hyperreactivity of mice to increasing doses of methacholine was measured by Flexivent (B) and total leukocytes (C), eosinophils (D), and neutrophils (E) were counted in the BALF. Control mice received isotype control in the similar fashion. The data points are represented as mean ± SEM. $N = 8$ mice/group. $^{*}p < 0.05$; $^{**}p < 0.01$; $^{***}p < 0.001$ and $^{****}p < 0.0001$ compared with isotype control group as determined by the two-way ANOVA-Bonferroni test

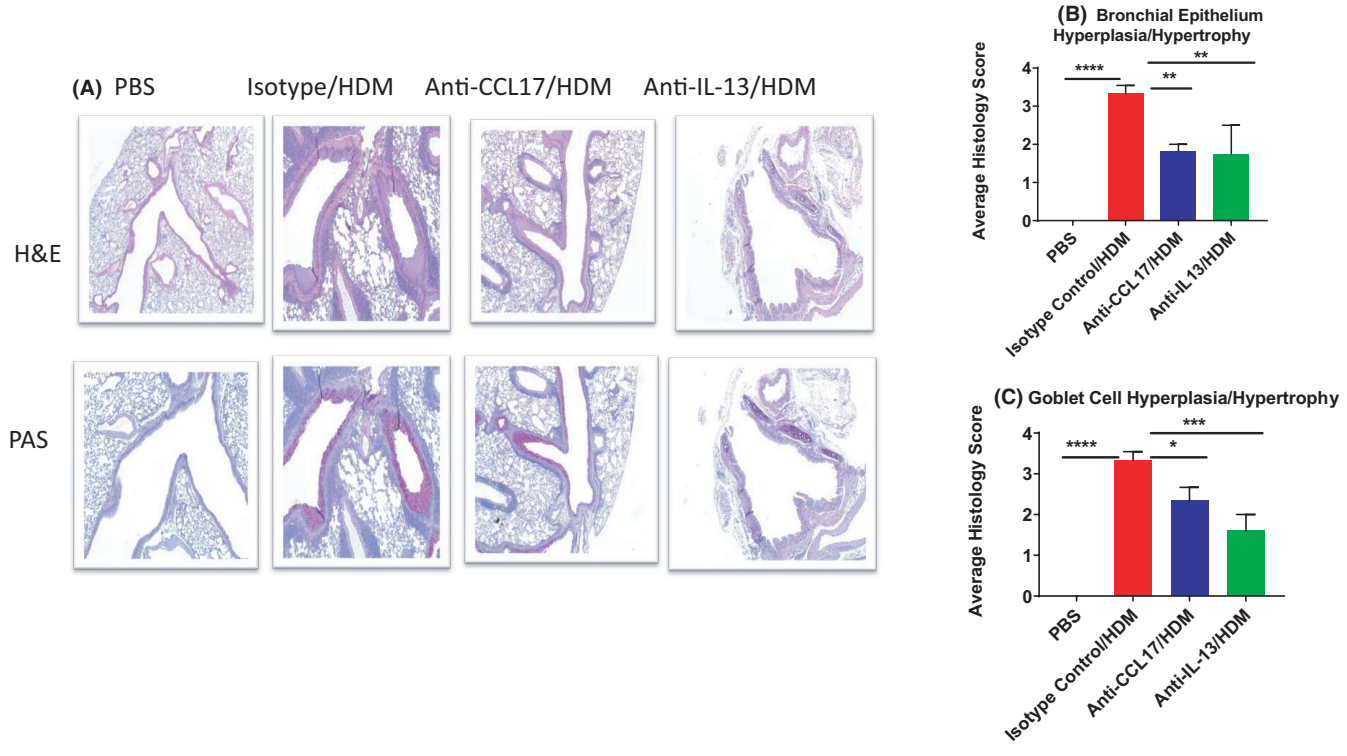

FIGURE 12 Effect of anti-CCL17 mAb on histopathological changes in HDM challenged mice. Mice were sensitized to PBS or HDM for 10 consecutive days (day 0–day 9). Lung tissues were obtained on day 11 and stained with H&E or PAS (A). Representative photomicrographs of airway sections are shown with 10× magnification. Lung sections were scored for histopathologic changes. Bronchiolar epithelial hyperplasia and hypertrophy (B) and increased goblet cell formation (C) were evaluated. The results are expressed on a scale of 0–5. The data points are represented as mean ± SEM. $N = 8$ mice/group. $^{*}p < 0.05$; $^{**}p < 0.01$ and $^{****}p < 0.001$ compared with isotype control group as determined by the two-way ANOVA-Bonferroni test

of HDM exposure and normalized during the resolution phase (day 21). These observations are similar to previous study that found an increase in Eotaxin-1, CXCL-1, IL-17A, IL-6, IL-4, IL-13, and IL-10 in a 14-day model.[18] The time course of cytokine/chemokine profile in BALF and lung tissue, that is, early appearance of TNFα, IL-17A, and KC, MCP-1 IL-10, and GM-CSF supports the notion that early lung inflammation is dominated by innate immune cells followed by Th2 dependent inflammation. Early appearance of TNFα, IL-17A, and KC coincided with the neutrophil influx.

IFNγ and IL-10 were postulated to initiate resolution of lung inflammation.[31,32] Thus, the appearance of IFNγ in the BAL/lung tissue and expression of IL-10 genes may have a role in inflammation resolution.

Gene expression analysis in BAL cells and lung tissue revealed significant, time-dependent upregulation of several genes (differentially expressed [DE] genes implying complex interplay between multiple cell types/chemokines and cytokines. Among these DE, *CLCA3* was the most highly expressed gene, expressed early and remained elevated during the HDM exposure. IL-13 is a known inducer of *CLCA3*[33] as well as *FOXA3*.[34] Both *FOXA3* and *CLCA3* are known to drive goblet cell hyperplasia.[35,36] In our study, goblet cell hyperplasia and hypertrophy were observed at the histological level.

HDM exposure led to marked tissue inflammation accompanied by structural changes as evidenced by histopathology and supported by increases in soluble collagen and TIMP-1 in the lung tissue. While we observed remodeling, clear fibrotic changes were not observed under the experimental conditions which likely require much longer period of HDM exposure, that is, 5–8 weeks.[18] In our study, while cellular influx and cytokine surge was largely resolved by day 21, the histopathology changes were still detected by day 21 implying distinct time course profiles.

The levels of IL-33 remained significantly elevated during and after HDM exposure. IL-33, which is highly expressed by the epithelial cells, initiates innate immune responses in mucosa acts on group 2 innate lymphoid cells (ILC2s) to produce Th2 cytokines such as IL-5 and IL-13. Additionally, IL-33 acts on dendritic cells, Th2 cells, follicular T cells, and regulatory T cells driving the adaptive responses, and thus orchestrates the development of chronic airway inflammation and tissue remodeling.[37] Higher levels of IL-33 have been detected in the lung of asthmatics,[38,39] and polymorphisms in the *IL-33* and *st2* genes are linked to higher incidence of allergic disease and asthma.[40]

The profound inflammatory and structural changes in the lungs of HDM challenged mice were associated with enhanced AHR to inhaled methacholine in HDM. AHR responses increased by day 11 and greatly decreased by day 21. These results are in agreement with previous studies employing varying HDM exposure paradigms.[41,42]

Murine models of allergic airway inflammation such as the OVA model of Th2 lung inflammation have enabled hypothesis testing and increased our understanding of the pathogenesis of asthma. The OVA model, while useful, lacks construct validity both in the route of administration and the acute nature of the challenge. Moreover passive respiratory exposure to OVA leads to inhalation tolerance.[43–46] Multiple variations of the HDM induced lung inflammation have been reported in the literature which differ in dose, duration of exposure, challenge paradigm, species and strains of animals used.[18,24,47–49] Incidentally, many of these studies have largely focused on characterization of inflammation at the end of HDM exposure. The present investigation provides a detailed temporal characterization of evolution of inflammation and its pharmacology. It is hoped that the results presented here are of topical interest to investigators studying aeroallergen induced allergy and atopy and their pharmacological modulation. At a more global level, the detailed time course of gene expression analysis conducted here provides for a deeper understanding of the evolution and resolution of pulmonary inflammation and pathways involved. HDM is a known human aeroallergen and as such, HDM induced lung inflammation models and characterization such as the one conducted here could help in translational research.

The chemokine receptor, CCR4 is highly expressed on Th2 cells and plays a key role in Th2 T cell recruitment into the asthmatic airways.[50,51] CCL17 and macrophage-derived chemokine (MDC)/CCL22 are known ligands of CCR4 and are up-regulated in the lungs of patients with allergic asthma[52] after rhinovirus infection[53] and COPD.[54]

The role of CCR4 and its ligands CCL17 and CCL22 in allergic disease is well established,[42–48] with the drug discovery efforts focused heavily on receptor antagonism ether with small molecules or mAbs. In addition, CCR4 signaling via CCL-17 has emerged as an attractive option to treat immune-inflammatory conditions driven by GMCSF.[55] Since nearly all Tregs express and use CCR4 receptor[56] for homing into sites of inflammation, CCR4 receptor blockade while attenuating inflammation may impact homeostatic resolution mechanisms. In this regard, targeting of CCL17 blockade is likely to spare Treg function while modulating Th2 recruitment.

Neutralization of MDC or CCL-17 attenuated ovalbumin (OVA)-induced Th2 lung inflammation.[45,57]. A TARC-PE38, a TARC fused exotoxin fragment PE38 from *Pseudomonas aeruginosa* has been shown to efficiently suppressed allergic airway inflammation by significantly reducing airway hyper-responsiveness, airway inflammation, and goblet cell hyperplasia by reducing $CD4^+$ cells.[58] A CCR4 neutralizing antibody leading to reduced levels of Th2 cytokines in the lungs of humanized severe combined immunodeficient mice harboring immune cells from allergic asthma patients.[59] The effects of a CCL17 mAb reduced BAL cellularity, eosinophilia, airway hyper-responsiveness, and goblet cell and epithelial hyperplasia in the present investigation further substantiate the role of CCL17 as mediator of inflammation driven by HDM.

In summary, the present investigation carefully characterized lung inflammation in response to repeated exposure to HDM. CCL-17 neutralization in this model led to marked anti-inflammatory effects that are accompanied by reduced airway hyper reactivity. Although, many pharmacological treatments for asthma and allergy have been evaluated, very few have been explored HDM-induced allergy and asthma in animal models and human. Furthermore, exploration of underlying mechanisms associated with HDM induced allergic asthma has been hampered in part due to the unavailability of specific biomarkers relevant

to human asthma. The data presented here further provides foundation to explore cellular and molecular basis of allergen induced immunopathology and potential to identify novel pharmacological interventions to evaluate prospective newer modalities. Finally, given the emerging role of CCL17:CCR4 signaling as a driver of several inflammatory conditions, CCL17 neutralization may provide anti-inflammatory activity while sparing the homeostatic Treg mediated immune modulation.

ACKNOWLEDGMENTS

The authors thank Heather Deutsch for histopathological analysis.

DISCLOSURE

Authors are/were employees of Janssen Research and Development. There are no other conflicts of interest.

AUTHORS CONTRIBUTIONS

RM, MR, and TR contributed to study conceptualization, data analysis, interpretation, and manuscript preparation. ZZ, HR, JW, BJ, RB, PW, and LH contributed to experimental conduct, methods, and initial data analysis. LM contributed to mRNA data analysis. RM and TR contributed to manuscript revision/finalization. All authors had access to the data and reviewed the manuscript.

ETHICS STATEMENT

All animal experiments were conducted in accordance with the policies of the Institutional Care and Use Committee (IACUC) of Janssen R&D and studies were conducted in an AAALAC accredited vivarium.

DATA AVAILABILITY STATEMENT

The data that support the findings of this study are available from the corresponding author upon reasonable request.

ORCID

Ravi Malaviya https://orcid.org/0000-0002-7020-9163

Tadimeti S. Rao https://orcid.org/0000-0001-5332-7304

REFERENCES

1. O'Byrne PM, Inman MD. Airway hyperresponsiveness. *Chest*. 2003;123(3):411S-416S.
2. Barnes PJ. The cytokine network in asthma and chronic obstructive pulmonary disease. *J Clin Invest*. 2008;118(11):3546-3556.
3. Holgate ST. Innate and adaptive immune responses in asthma. *Nat Med*. 2012;18(5):673-683.
4. Kim HY, DeKruyff RH, Umetsu DT. The many paths to asthma: phenotype shaped by innate and adaptive immunity. *Nat Immunol*. 2010;11(7):577-584.
5. Wenzel SE. Asthma phenotypes: the evolution from clinical to molecular approaches. *Nat Med*. 2012;18(5):716-725.
6. Zock J, Heinrich J, Jarvis D, et al. Distribution and determinants of house dust mite allergens in Europe: the European Community Respiratory Health Survey II. *J Allergy Clin Immunol*. 2006;118(3):682-690.
7. Arshad SH. Does exposure to indoor allergens contribute to the development of asthma and allergy? *Curr Allergy Asthma Rep*. 2010;10(1):49-55.
8. Yahia SA, Azzaoui I, Everaere L, et al. CCL17 production by dendritic cells is required for NOD1-mediated exacerbation of allergic asthma. *Am J Respir Crit Care Med*. 2014;189(8):899-908.
9. Fukuda K, Fujitsu Y, Seki K, et al. Differential expression of thymus- and activation-regulated chemokine (CCL17) and macrophage-derived chemokine (CCL22) by human fibroblasts from cornea, skin, and lung. *J Allergy Clin Immunol*. 2003;111(3):520-526.
10. Hewitt CR, Foster S, Phillips C, et al. Mite allergens: significance of enzymatic activity. *Allergy*. 1998;53:60-63.
11. Keglowich L, Tamm M, Zhong J, et al. Proteolytic activity present in house-dust-mite extracts degrades ENA-78/CXCL5 and reduces neutrophil migration. *J Allergy*. 2014;2014:1-9.
12. Johnson JR, Wiley RE, Fattouh R, et al. Continuous exposure to house dust mite elicits chronic airway inflammation and structural remodeling. *Am J Respir Crit Care Med*. 2004;169(3):378-385.
13. Malaviya R, Chen CL, Navara C, et al. Treatment of allergic asthma by targeting janus kinase 3-dependent leukotriene synthesis in mast cells with 4-(3', 5'-dibromo-4'-hydroxyphenyl)amino-6,7-dimethoxyquinazoline (WHI-P97). *J Pharmacol Exp Ther*. 2000;295(3):912-926.
14. Harding SD, Sharman JL, Faccenda E, et al. The IUPHAR/BPS Guide to PHARMACOLOGY in 2018: updates and expansion to encompass the new guide to IMMUNOPHARMACOLOGY. *Nucleic Acids Res*. 2018;46(D1):D1091-D1106.
15. Alexander SPH, Kelly E, Mathie A, et al. THE CONCISE GUIDE TO PHARMACOLOGY 2019/20: introduction and other protein targets. *Br J Pharmacol*. 2019;176(Suppl 1):S1-S20.
16. Calderón MA, Kleine-Tebbe J, Linneberg A, et al. House dust mite respiratory allergy: an overview of current therapeutic strategies. *J Allergy Clin Immunol Pract*. 2015;3(6):843-855.
17. Calderón MA, Linneberg A, Kleine-Tebbe J, et al. Respiratory allergy caused by house dust mites: what do we really know? *J Allergy Clin Immunol*. 2015;136(1):38-48.
18. Woo LN, Guo WY, Wang X, et al. A 4-week model of house dust mite (HDM) induced allergic airways inflammation with airway remodeling. *Sci Rep*. 2018;8(1):6925.
19. Huang FL, Liao EC, Yu SJ. House dust mite allergy: its innate immune response and immunotherapy. *Immunobiology*. 2018;223(3):300-302.
20. John RJ, Rusznak C, Ramjee M, Lamont AG, Abrahamson M, Hewitt EL. Functional effects of the inhibition of the cysteine protease activity of the major house dust mite allergen Der p 1 by a novel peptide-based inhibitor. *Clin Exp Allergy*. 2000;30(6):784-793.
21. Osterlund C, Grönlund H, Polovic N, et al. The non-proteolytic house dust mite allergen Der p 2 induce NF-kappaB and MAPK dependent activation of bronchial epithelial cells. *Clin Exp Allergy*. 2009;39(8):1199-1208.
22. Pineiro-Hermida S, Alfaro-Arnedo E, Gregory JA, et al. Characterization of the acute inflammatory profile and resolution of airway inflammation after Igf1r-gene targeting in a murine model of HDM-induced asthma. *PLos One*. 2017;12(12):e0190159.
23. Post S, Nawijn MC, Hackett TL, et al. The composition of house dust mite is critical for mucosal barrier dysfunction and allergic sensitisation. *Thorax*. 2012;67(6):488-495.
24. Bracken SJ, Adami AJ, Szczepanek SM, et al. Long-term exposure to house dust mite leads to the suppression of allergic airway disease despite persistent lung inflammation. *Int Arch Allergy Immunol*. 2015;166(4):243-258.
25. de Boer JD, Berger M, Majoor CJ, et al. Activated protein C inhibits neutrophil migration in allergic asthma: a randomised trial. *Eur Respir J*. 2015;46(6):1636-1644.
26. Berger M, de Boer JD, Bresser P, et al. Lipopolysaccharide amplifies eosinophilic inflammation after segmental challenge with house dust mite in asthmatics. *Allergy*. 2015;70(3):257-264.
27. Chesné J, Braza F, Chadeuf G, et al. Prime role of IL-17A in neutrophilia and airway smooth muscle contraction in a house dust

mite-induced allergic asthma model. *J Allergy Clin Immunol*. 2015;135(6):1643-1645.e5.
28. Moynihan BJ, Tolloczko B, El Bassam S, et al. IFN-gamma, IL-4 and IL-13 modulate responsiveness of human airway smooth muscle cells to IL-13. *Respir Res*. 2008;9:84.
29. Wills-Karp M, Luyimbazi J, Xu X, et al. Interleukin-13: central mediator of allergic asthma. *Science*. 1998;282(5397):2258-2261.
30. Tachdjian R, Al KS, Schwinglshackl A, et al. In vivo regulation of the allergic response by the IL-4 receptor alpha chain immunoreceptor tyrosine-based inhibitory motif. *J Allergy Clin Immunol*. 2010;125(5):1128-1136 e1128.
31. Lajoie S, Lewkowich IP, Suzuki Y, et al. Complement-mediated regulation of the IL-17A axis is a central genetic determinant of the severity of experimental allergic asthma. *Nat Immunol*. 2010;11(10):928-935.
32. Pineiro-Hermida S, Gregory JA, Lopez IP, et al. Attenuated airway hyperresponsiveness and mucus secretion in HDM-exposed Igf1r-deficient mice. *Allergy*. 2017;72(9):1317-1326.
33. Hall SL, Baker T, Lajoie S, et al. IL-17A enhances IL-13 activity by enhancing IL-13-induced signal transducer and activator of transcription 6 activation. *J Allergy Clin Immunol*. 2017;139(2):462-471.e14.
34. Chen G, Korfhagen TR, Karp CL, et al. Foxa3 induces goblet cell metaplasia and inhibits innate antiviral immunity. *Am J Respir Crit Care Med*. 2014;189(3):301-313.
35. Leverkoehne I, Gruber AD. The murine mCLCA3 (alias gob-5) protein is located in the mucin granule membranes of intestinal, respiratory, and uterine goblet cells. *J Histochem Cytochem*. 2002;50(6):829-838.
36. Mushaben EM, Brandt EB, Hershey GK, et al. Differential effects of rapamycin and dexamethasone in mouse models of established allergic asthma. *PLoS One*. 2013;8(1):e54426.
37. Zoltowska Nilsson AM, Lei Y, Adner M, et al. Mast cell-dependent IL-33/ST2 signaling is protective against the development of airway hyperresponsiveness in a house dust mite mouse model of asthma. *Am J Physiol Lung Cell Mol Physiol*. 2018;314(3):L484-L492.
38. Raeiszadeh JS, Mahesh PA, Jayaraj BS, et al. Serum levels of IL-10, IL-17F and IL-33 in patients with asthma: a case-control study. *J Asthma*. 2014;51(10):1004-1013.
39. Préfontaine D, Lajoie-Kadoch S, Foley S, et al. Increased expression of IL-33 in severe asthma: evidence of expression by airway smooth muscle cells. *J Immunol*. 2009;183(8):5094-5103.
40. Zoltowska AM, Lei Y, Fuchs B, et al. The interleukin-33 receptor ST2 is important for the development of peripheral airway hyperresponsiveness and inflammation in a house dust mite mouse model of asthma. *Clin Exp Allergy*. 2016;46(3):479-490.
41. Cates EC, Fattouh R, Johnson JR, et al. Modeling responses to respiratory house dust mite exposure. *Contrib Microbiol*. 2007;14(suppl 17684332):42-67.
42. Piyadasa H, Altieri A, Basu S, et al. Biosignature for airway inflammation in a house dust mite-challenged murine model of allergic asthma. *Biol Open*. 2016;5(2):112-121.
43. Holt PG, Batty JE, Turner KJ. Inhibition of specific IgE responses in mice by pre-exposure to inhaled antigen. *Immunology*. 1981;42(3):409-417.
44. McMenamin C, Pimm C, McKersey M, et al. Regulation of IgE responses to inhaled antigen in mice by antigen-specific gamma delta T cells. *Science*. 1994;265(5180):1869-1871.
45. Seymour BW, Gershwin LJ, Coffman RL. Aerosol-induced immunoglobulin (Ig)-E unresponsiveness to ovalbumin does not require $CD8^+$ or T cell receptor (TCR)-gamma/delta+ T cells or interferon (IFN)-gamma in a murine model of allergen sensitization. *J Exp Med*. 1998;187(5):721-731.
46. Swirski FK, Gajewska BU, Alvarez D, et al. Inhalation of a harmless antigen (ovalbumin) elicits immune activation but divergent immunoglobulin and cytokine activities in mice. *Clin Exp Allergy*. 2002;32(3):411-421.
47. Abbring S, Verheijden KAT, Diks MAP, et al. Raw cow's milk prevents the development of airway inflammation in a murine house dust mite-induced asthma model. *Front Immunol*. 2017;8:1045.
48. Nazir R, Khanna M, Kulshrestha R. Time course of pulmonary pathology, cytokine influx and their correlation on augmentation of antigen challenge by influenza A virus infection. *Indian J Exp Biol*. 2008;46(3):151-158.
49. Maeda S, Maeda S, Shibata S, et al. House dust mite major allergen Der f 1 enhances proinflammatory cytokine and chemokine gene expression in a cell line of canine epidermal keratinocytes. *Vet Immunol Immunopathol*. 2009;131(3-4):298-302.
50. Bussmann C, Maintz L, Hart J, et al. Clinical improvement and immunological changes in atopic dermatitis patients undergoing subcutaneous immunotherapy with a house dust mite allergoid: a pilot study. *Clin Exp Allergy*. 2007;37(9):1277-1285.
51. Maneechotesuwan K, Wongkajornsilp A, Huabprasert S, et al. Differential expression of Th2 chemokine receptors on T cells from atopic and nonatopic asthmatics in response to Der p 1-pulsed dendritic cells. *J Med Assoc Thai*. 2010;93(Suppl 1):S62-S70.
52. Pilette C, Francis JN, Till SJ, et al. CCR4 ligands are up-regulated in the airways of atopic asthmatics after segmental allergen challenge. *Eur Respir J*. 2004;23(6):876-884.
53. Williams TC, Jackson DJ, Maltby S, et al. Rhinovirus-induced CCL17 and CCL22 in asthma exacerbations and differential regulation by STAT6. *Am J Respir Cell Mol Biol*. 2021;64(3):344-356.
54. Machida H, Inoue S, Shibata Y, et al. Thymus and activation-regulated chemokine (TARC/CCL17) predicts decline of pulmonary function in patients with chronic obstructive pulmonary disease. *Allergol Int*. 2021;70(1):81-88.
55. Lee KM, Jarnicki A, Achuthan A, et al. CCL17 in Inflammation and Pain. *J Immunol*. 2020;205(1):213-222.
56. Hirahara K, Liu L, Clark RA, et al. The majority of human peripheral blood $CD4^+$ CD25 high $Foxp^{3+}$ regulatory T cells bear functional skin-homing receptors. *J Immunol*. 2006;177(7):4488-4494.
57. Gonzalo JA, Pan Y, Lloyd CM, et al. Mouse monocyte-derived chemokine is involved in airway hyperreactivity and lung inflammation. *J Immunol*. 1999;163(1):403-411.
58. Honjo A, Ogawa H, Azuma M, et al. Targeted reduction of $CCR4^+$ cells is sufficient to suppress allergic airway inflammation. *Respir Investig*. 2013;51(4):241-249.
59. Perros F, Hoogsteden HC, Coyle AJ, et al. Blockade of CCR4 in a humanized model of asthma reveals a critical role for DC-derived CCL17 and CCL22 in attracting Th2 cells and inducing airway inflammation. *Allergy*. 2009;64(7):995-1002.

SUPPORTING INFORMATION

Additional supporting information may be found online in the Supporting Information section.

How to cite this article: Malaviya R, Zhou Z, Raymond H, et al. Repeated exposure of house dust mite induces progressive airway inflammation in mice: Differential roles of CCL17 and IL-13. *Pharmacol Res Perspect*. 2021;9:e00770. https://doi.org/10.1002/prp2.770